The Measurement Of Microwave Emissivities Of Arid And Verdant Land Types In The Crau-Camargue Region Of France

K. Foster , T. Hewison

The author is with the UK Meteorological Office,
Y70,DERA Farnborough, Hants, GU14 0LX, UK. email: KFOSTER@meto.gov.uk

ABSTRACT

The Crau-Camargue airborne experiment took place between the 10th and the 14th of July 1995 on the south coast of France. The purpose of the experiment was to measure microwave for a number of arid and verdant land types as found in the region. The UK meteorological C-130 aircraft participated, taking measurements with its two microwave radiometers, MARSS and Deimos, and with a multi-channel infa-red (Ir) radiometer, SAFIRE. Results are presented on the microwave emissivities spectra of verdant and arid land types.

Keywords: Microwave surface emissivity, Arid, Verdant, Airborne

1. INTRODUCTION

In order to use microwave satellite sounding data to retrieve temperature and humidity profiles, it is important to know the emissivity and scattering properties of the underlying surface. As part of its continuing effort into measuring the microwave characteristics of different surface types, the UK Meteorological Office (UKMO) organised the Crau-Camargue airborne experiment in collaboration with Meteo-France, CETP and INRA of France. The experiment was based at Istres le Tube airfield on the French south coast (see map in figure 1), and took place between the 9th and 14th of July 1995. During this period three scientific sorties were flown over the Crau and Camargue regions.

The Camargue region is mainly agricultural where a wide variety of vegetation and surface types, from rice paddys to bare ploughed earth, can be found. Samples of each of these many land types were overflown during each sortie, though the majority of the data that was obtained was for verdant crops.

The Crau region, which lies to the North East of Istres, is entirely different in nature being made up mainly of large areas of arid plane and scrub. This region was also extensively overflown during the three sorties.

This report is concerned with the data collected by the UKMO C-130 aircraft and its onboard radiometers. The measurement of the microwave emissivity of representative arid and agriculturally verdant surfaces will be investigated.

2. INSTRUMENTS

The UKMO C-130 carries a wide range of meteorological and navigational instruments. For the purpose of this experiment the most important were the two microwave radiometers, MARSS and Deimos, the multi-channel Ir radiometer, SAFIRE, and the broader band thermal Ir Heimman radiometer.

MARSS and Deimos are both total power radiometers with along track scans of 3 seconds. Deimos has channels at 24GHz and 50GHz and has five downward views from -5° to 35° from nadir. It measures two polarizations for each of the channels which are aligned to V and H in the far forward field of view and are mixed in the nadir. During the experiment a problem arose with the the polarization of the 50GHz channel that noticeable differences between the two polarizations in the nadir view. The scale of this problem is not too large and any effect it has will be considered later. MARSS has channels at 89GHz and 157GHz, with nine upward and nine downward views. Both instruments are calibrated with respect to two internal black body targets which they view once a scan. Table 1 details their performance during the period of this experiment. Unfortunately problems arose with MARSS which meant that no microwave zenith data would be available for any of the flights. This problem and its impact on the calculation of emissivity are discussed later in section 4 and in the conclusions. For a more full description of these instruments see ref. (1) and ref(2).

SPIE Vol. 3220 • 0277-786X/98/$10.00

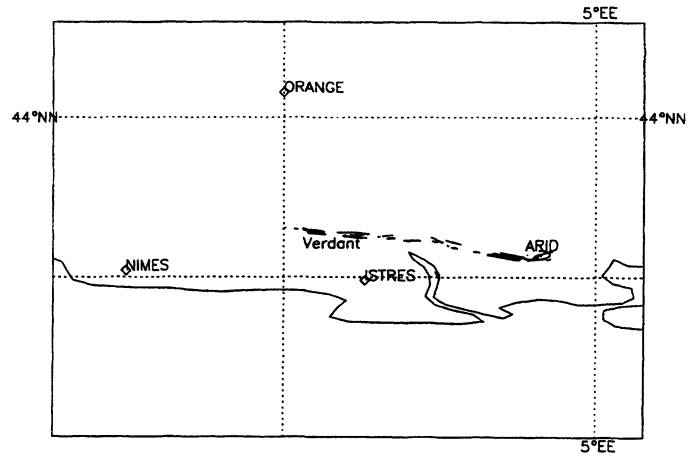

Figure 1. Map of Crau and Camargue regions, with fight paths marked on for the 11th and 13th.

The SAFIRE instrument has four channels that can be selected from a wavelength range of 0.62μm to 12μm .The wavelengths are set by means of a filter wheel which has, at one setting, channels at 0.62μm, 1.25μm, 11μm and 12μm. The 0.62μm and 1.25μm channels can be used to calculate a vegetation index similar to the normalised difference vegetation index (NDVI), whilst the 11μm and 12μm channels can be used to measure the surface temperature. It should be noted that the derived vegetation index is different from the NDVI due to the different frequencies used to calculate it. During the experiment several filter wheel settings were used, which meant that vegetation index data was no available for a lot of the time. SAFIRE views across track at a range of angles from -5° to 60° and has two internal blackbody targets for calibration.

The Heimman radiometer is used for measuring the surface temperature and has response to radiation of a wavelengths between 8μm and 15μm. This is quite a broad wavelength band and as such the surface temperature measured tends to be effected by atmospheric absorption. The values derived for the surface temperature from the Heimman have been compared with the SAFIRE 11μm and 12μm channels, which are less effected by atmospheric absorption , and they give good agreement for low levels runs.

A set of upward and downward hemispherical pyranometers were also available on the aircraft and are referred to as broad band radiometers (BBR). One of the BBRs has a clear filter with a response to radiation of wavelengths between 0.3μm and 3μm .This was used during the experiment to indicate the degree of cloud cover above the aircraft, and is discussed in section 4.1 .

The C-130 also has downward and forward facing video cameras. Video footage from the downward facing camera was available for all of the flights and greatly aided surface classification. The footage from the forward facing camera is very useful in determining the amount of cloud cover present, which is important in radiometric surface measurement campaigns. A full set of standard meteorological instruments, from which atmospheric temperature and humidity profiles can be measured, are also available.

3. FLIGHTS SUMMARY

Three scientific sorties were made during the experiment each of which overflew the same areas. The flight paths for the aircraft over the regions of interest on the 11th, flight A395, and the 13th, flight A397, are shown on the map in figure 1. The flight pattern for each sortie changed little on a day to day basis and consisted of straight and level runs over the land at 500, 1000 and 2000 feet, with profiles from near the surface (500 feet over land and 100 feet over the sea) to high levels (25,000 feet) in order to measure atmospheric temperature and humidity profiles. Meteorological

Table 1. Summary of Radiometer Systems

Aircraft	UKMO C-130			
Instrument	Deimos		MARSS	
Frequency /GHz	23.8	50.1	89.0	157.0
View angle	+35° to -5° Down only		+40° to -40° Up and Down	
Scan period	3s		3s	
Beamwidth (3dB)	11°		10°	
Polarisation Crau	V,H	V,H	Mixed	V or H
Integration time	50ms	50ms	80ms	80ms
Sensitivity, ΔT	0.6K	0.6K	0.3K	0.5K
Absolute Accuracy	1.4K	1.7K	3.5K	4.0K

conditions during the experiment were far from ideal, with substantial ammounts of cloud cover present on most days.

During the 11th the cloud cover varied from 7/8 to 1/8 Cumulus and during the afternoon thunderstorms with 2.2mm of rain were recorded at the meteorological stations at Nimes and Orange (see figure 1). The conditions on the 12th were much clearer but due to instrument failures little data was recorded. On the 13th it was again cloudy, but less so than on the 11th, with amounts varying from 1/8 to 4/8 Cumulus. Because of the loss of data on the 12th, only the flights on the 11th and 13th will be considered.

4. CALCULATION OF SURFACE EMISSIVITY

The emissivity of a surface is calculated from the nadir and zenith observed brightness temperatures and the thermodynamic surface temperature by the following formula ;

$$\epsilon(\nu,\theta) = \frac{T_n(\nu,\theta) - T_z(\nu,\theta)}{T_s - T_z(\nu,\theta)} \tag{1}$$

where, ϵ, is the emissivity at frequency, ν, and angle of incidence, θ; T_z, the zenith brightness temperature at the surface; T_n, the emitted surface brightness temperature and, T_s, the surface temperature. Either a diffuse or a specular emissivity can be calculated for any particular surface, as to which is the more relevant depends on the nature of the surface. Since most of the land surfaces encountered during this experiment were Lambertian in nature all the surface emissivities were calculated as diffuse, which is done by using the downwelling hemispherical average brightness temperature for T_z.

4.1. Downwelling Brightness Temperatures

The absence of MARSS zenith data required that the downwelling brightness temperature be calculated from a radiative transfer model (Liebe '93), which has in the past been shown to be accurate at the MARSS and Deimos Frequencies when modelling clear and cloudy skies (see ref.(2)). Usually the zenith brightness temperatures at 24GHz and 50GHz (the frequencies corresponding to Deimos) are derived from the MARSS ones, but in this case the same radiative transfer model was used to calculate them.

The atmospheric temperature and humidity profiles that are required for the running of the model were obtained from an aircraft profile. An aircraft profile was used in preference of profiles from a radiosonde ascent because it was felt to be more representative of the variable local conditions.

The errors in the model vary with the amount of liquid water present. For the amounts measured on the 11th and the 13th, 3mm to 4mm, the errors are of the order of 4K for the 89GHz and 157GHz channels (see ref (2)). The errors for the 24GHz and the 50GHz channels have been have been measured as 1.4K and 3.4K for a clear sky

case (see ref (3)), though no measurement of how they vary with increasing liquid water content was available at the time of writing. It was therefore decided to use zenith brightness temperatures that were modelled without any cloud to replace the missing data. Using a scaled mix of clear and cloudy model zenith brightness temperatures was considered but it was thought that this would introduce as much uncertainty as it sought to dispel, even at the low frequency channels that are less effected by cloud. Hence a means of flagging cloudy views was required, and to this end the upper clear BBR was used. The flagging of cloud contaminated views was acheived by comparing the downward flux from the clear B.B.R. with that calculated from a semi-empirical model. Figure 2 shows the recorded clear flux for the flight on the 11th with the calculated values overplotted.

In order to measure the effect that cloud would have on the calculated zenith brightness temperatures, and the resultant maximum tolerable degree of cloud cover, the clear and cloudy model outputs were compared. From analysis of the differences between the two cases it was seen that the channel that was worst effected by cloud in its zenith field of view was 157GHz, as can be seen in figure 3. A zenith error was derived from the above method by using a simple mixing of the clear and cloudy cases to represent realistic amounts of cloud.

4.2. Errors In The Emissivity

A plot of the errors in the emissivity, as calculated from the uncertainty in the zenith and nadir brightness temperatures and the surface temperature, for each of the frequencies is shown in figure 3. The plot of the brightness temperature errors alongside it was calculated for a typical low-level run over a surface of a relatively low emissivity (e = 0.7). These are the absolute errors for each of the frequencies, and from these we can quote a range of scene temperatures for which the surface emissivity can be calculated with any certainty and this region of moderate error lies between surface temperatures of 290K and 320K. It is apparent that the 157GHz channel is effected far more than the others by the uncertainty in the zenith brightness temperatures and this tends to cast doubts on the use of modelled zenith brightness temperatures at this channel for any but the clearest of skies.

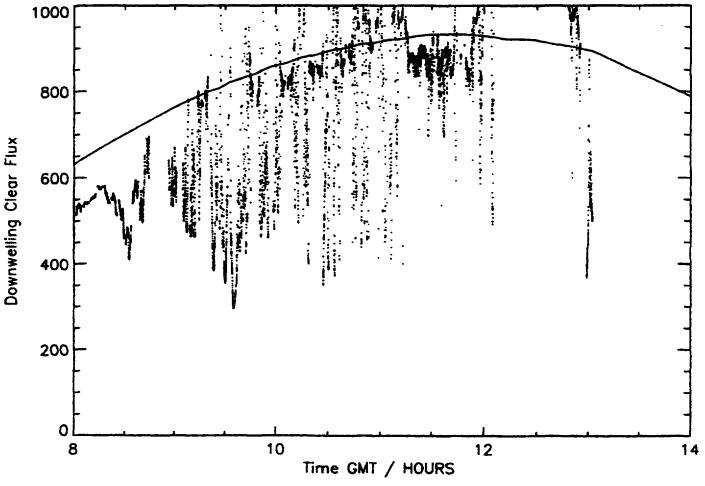

Figure 2. A plot of the down-welling radiant flux between 0.3μm and 3μm .

4.3. Atmospheric Correction

In order to calculate the emissivity it is necessary to correct for the atmospheric absorption of the air beneath the aircraft. Radiative transfer models were used (Liebe'93 for the microwave and MODTRAN for the Ir) to calculate the transmitivity of 1200 standard atmospheric profiles. From these, coefficients were then derived relating the optical depth of a portion of a profile, from the surface up to a particular pressure level, to the pressure and humidity at that level. They were then used to correct the microwave and Ir brightness temperatures to those at the surface. For a full description of the method of producing emissivities for these two instruments see ref. (4).

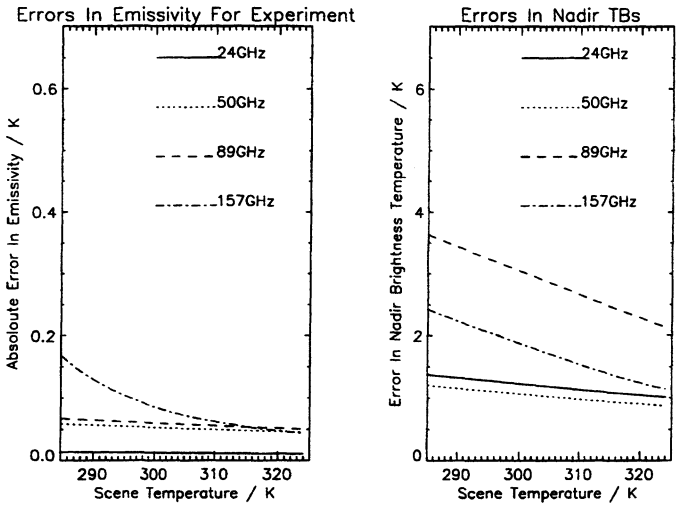

Figure 3. Emissivity and brightness temperature errors for each channel.

4.4. IR Emissivity Correction

In the calculation of the microwave surface emissivity, no allowance for the Ir emissivity of the surface (and therefore for the inaccuracy in the measured surface temperature) has been made. All the figures quoted in this report are for effective emissivities. The lowest Ir emissivity that would be encountered in these regions is that for sand. Sand has a measured Ir emissivity of 0.9 (see ref. (5)) which results in a large error in the microwave emissivity of the order of 0.2 for 24GHz and as high as 0.35 for 50GHz and 89GHz. Any regions containing appreciable amounts of sand should become apparent from comparing the microwave emissivities, the surface temperature and the downward video footage.

5. ANALYSIS OF DATA FROM THE ARID CRAU REGION

Extensive runs over the Crau region were made on both the 11th and the 13th of July. The arid plain that was overflown was several kilometers in length and appeared, from the downward looking video footage, to be relatively homogenous. On the video it appears as easily identified light brown to red areas. Photographs of the area taken in advance of the experiment showed it to be made mainly of a mix of bare earth and very short parched grass.

The surface temperature of this arid region was measured by the Heimman radiometer at 311 +/- 0.9 K (38° C) during the morning of the 13th, and the low standard deviation is indicative of the homogeneity of the surface during these runs. Analysis of the flight video was able to identify 12 separate runs for the sortie on the 11th and 9 for the sortie on the 13th, totalling about 10 minutes in all. Emissivities were calculated for each of the runs and the averages for the flight on the 13th are shown in the table below. The data from the flight on the 11th was found to be too contaminated by cloud to be of any use.

Table 2. Average & Standard Deviation of Nadir Emissivities for Arid Land

Category	$\epsilon(24)$	$\sigma\,\epsilon(24)$	$\epsilon(50)$	$\sigma\,\epsilon(50)$	$\epsilon(89)$	$\sigma\,\epsilon(89)$	$\epsilon(157)$	$\sigma\,\epsilon(157)$
Nadir Arid	0.917	0.011	0.945	0.008	0.958	0.004	0.967	0.006

The values for the 89GHz and the 157GHz channels are noticeably high and this is most probably due to the zenith brightness temperatures being larger than the modelled ones used at these frequencies. The largest likely bias

of the emissivity that could be cause by cloud is 0.01 for 157GHz and 0.005 for the other channels which are less effected by cloud. Nevertheless the overall trend is apparent, even if it is slightly inflated at the higher frequencies. A Spectrum of the nadir data collected over the arid region is shown in figure 4, and it has a line fit based on a Grody surface paramatization overplotted, which is discussed later. Artificial noise has been added to the frequency axes in order to show up any clustering of the data.

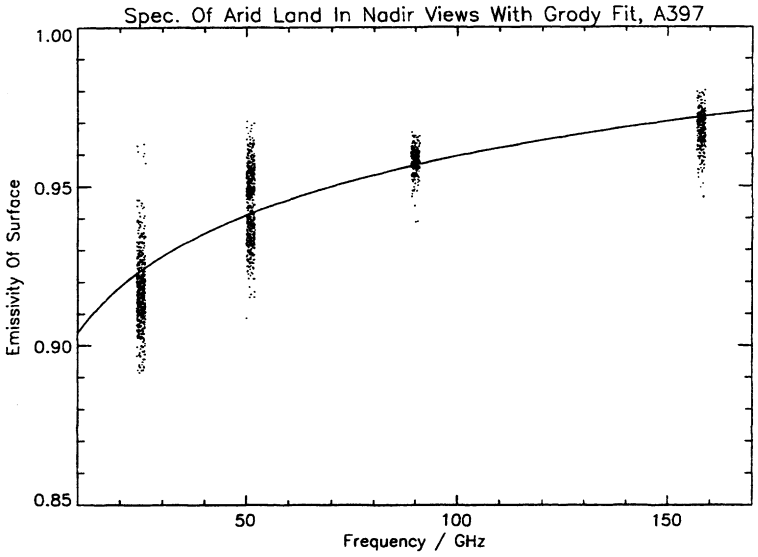

Figure 4. Emissivity spectra for arid regions

It can be seen form this plot, though it is much more evident in figure 5, that the 24GHz data is clustered into three distinct groups. A main group with an average emissivity of about 0.915 and a group above and one below. The apparent splitting of the 50GHz channel into two clusters is due to a systematic inaccuracy in one of the 50GHz polarisations, as was mentioned in section 2, and should not be taken as being important. If each polarisation is examined individually some sign of clustering is present but it is always less pronounced than it is for 24GHz.

The vegetation cover of the region was estimated using a vegetation index that is derived from two of the SAFIRE channels (see section 2). As would be expected the vegetation cover varied very little, values for the index were measured between -0.2 and -0.3, which we can compare to measured values of -0.6 for open water and 0.3 to 0.4 for lush vegetation. Plots of the 24GHz emissivity against the derived vegetation index and one of the 24GHz emissivity versus surface temperature are shown in figure 5. No discernible trend in the emissivities with surface temperature could be found for the arid regions, though this is unsurprising due to the lack of variation in this parameter. A trend can be seen in the emissivity with vegetation index, if the upper cluster is ignored and if the lower cluster is of the same land type and is not just mis-identified. These plots illustrate the clustering of the 24GHz data well.

It is possible that this clustering could be artificial and due to the use of modelled zenith brightness temperatures if the degree of cloud cover changed rapidly between stable amounts during the day. But this seems unlikely for it is most pronounced at the channel that is least effected by cloud. The higher cluster could represent areas with a higher than normal amount of sand. Such areas would have an underestimated surface temperature and hence an overestimated microwave emissivity. The vegetation index would seem to support this. The lower emissivity cluster could represent a volume scattering effect, since it can be seen at each frequency, or a mis-identification of the surface type. As yet we are unsure as to its nature.

There is significant polarization information available over this arid region, but only at 24GHz due to the polarization problem at 50GHz. Figure 6 shows the polarisation differences and averages for the 24GHz channel in the

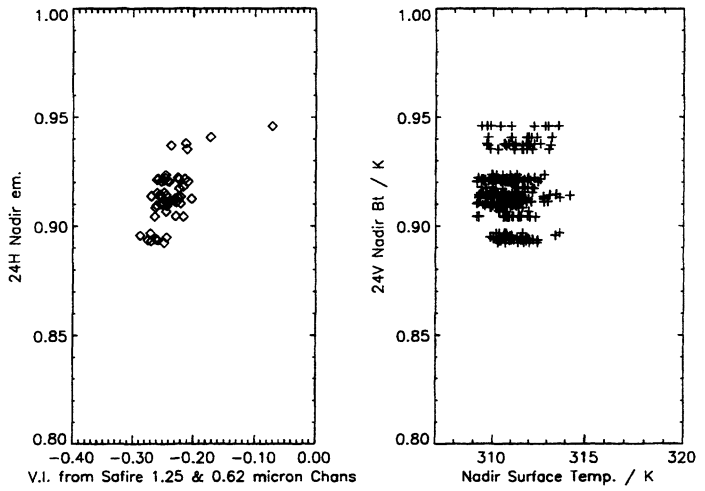

Figure 5. 24GHz emissivity against vegetation index and surface temperature.

forwad field of view and highlights the slow rate of change of the 24GHz emissivity with decreasing nadir emissivity.

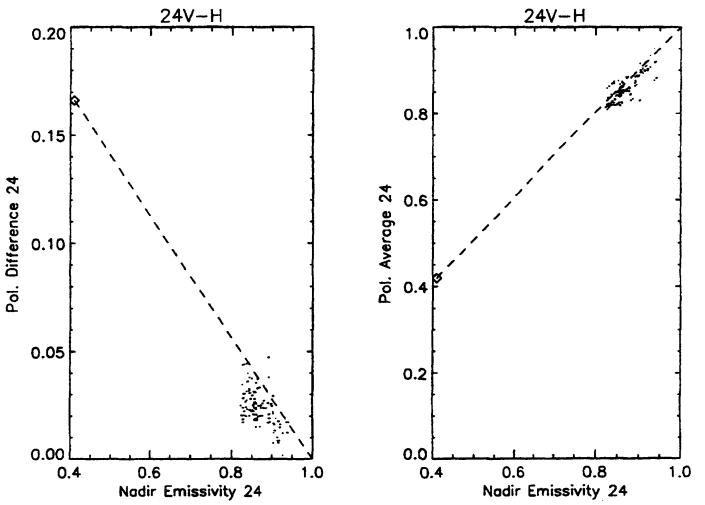

Figure 6. Polarisation information over arid surfaces

6. ANALYSIS OF THE VERDANT VEGETATION REGIONS

The Camargue region was overflown during each of the three scientific sorties. The region primarily consists of a patchwork of different vegetation and surface types each of which are relatively small in size. This proved problematic in analysising the aircraft data since most of the homogenous regions overflown were of too short a length to be useful. It was therefore decided to concentrate upon areas of verdant crop which were moderately extensive in area.

From the runs made on the 11th and the 13th of July, 13 minutes of data overflying fields containing dense, lush crop types were recorded .

From the available downward looking video camera footage the regions studied appear to be a mix of rice paddies, which sometimes had free water visible in them, and other dense verdant crops, such as soya and alfalfa . Identifying exactly which crops were which proved difficult due to the visual similarity of them and the difficulty of identifying free water from the video footage. Some measure of the degree of standing water present, which is useful in identifying rice crops, can be gained from the surface temperature and the nadir microwave brightness temperatures. The surface temperature was on average 300K across the majority of the verdant sites but it had a standard deviation that ranged from 40K to less than 1K on a site to site basis. Similarly, the average nadir 24GHz brightness temperature for a site could vary from 250k to 290k, with a maximum standard deviation of around 40K and a minimum of under 2K. It became apparent from the data that the crops could be roughly divided into two groups, one with low average brightness temperatures and high standard deviations and one with high averages and low standard deviations. It was therefore taken that there were two different types of land category present in the data, land type one and land type two, and that a filter based upon the above could be used to separate them.

Table 3, below, contains the average emissivities and the standard deviations for each of the defined two types, as calculated from the flight on the 11th and on the 13th. The spectra of the two categories have also been produced and are shown in figure 7.

Table 3. Average & Standard Deviation of Nadir Emissivities for Verdant Land

Category	$\epsilon(24)$	$\sigma\ \epsilon(24)$	$\epsilon(50)$	$\sigma\ \epsilon(50)$	$\epsilon(89)$	$\sigma\ \epsilon(89)$	$\epsilon(157)$	$\sigma\ \epsilon(157)$
Land Type 1	0.829	0.066	NA	NA	0.924	0.037	0.965	0.024
Land Type 2	0.939	0.027	0.948	0.035	0.947	0.033	0.977	0.020

It should be noted that the absence of 50GHz data for land type one is due to the problem with the plarization of this channel that was mentioned in section 2. This problem is somewhat cappraicous in nature effected all the data to the same extent. The 50GHz emissivitiy for land type two is relatively uneffected in that the emissivity is slightly higher than it should be, by quite how much is uncertain untill it is established which polarization is in error.

The first of the two spectra represents land type one, those with low and variable 24GHz brightness temperatures. A wide range of emissivities have been caught in this group and this would lead one to suspect that it in fact contains data from irrigated rice fields where the degree of free water is quite large and varies from field to field. The resultant emissivity measured would depend on the degree to which free water fills the field of view of the instrument, the volumetric content of liquid water in the soil and on the density of the crop cover. The second plot shows the spectra for land category two. The emissivities here are more well defined, with a range of approximately 0.1. They are consistently high and most likely represent dense vegetation over relatively a dry soil (probably no more than 30ref (6)). From the above data it would appear that the emissivity of these verdant regions is dominated by the amount of free water present.

A vegetation index was derived for the sites using the SAFIRE instrument, and a plot of the vegetation index versus the 24GHz emissivity, as well as one of vegetation index versus surface temperature, is shown in figure 8. These plots contain data from verdant regions. It is worth pointing out that Deimos and SAFIRE have very different beamwidths, SAFIRE has a beam of only 2.5° compared to 11° for Deimos. So this coupled with the small amount of SAFIRE data available, and the intrinsic spatial variabilty of the irrigated crops, makes it difficult to distinguish between outliers and actual relationships in the gegetation data. A wide spread of the vegetation index is seen in the first plot, but the majority of points have a index of between 0.0 and 0.5 which is consistent for dense crops. The second plot alongside it shows the relationship between vegetation index and the surface temperature. There is a clear linear dependence for the majority of points with two groups, one to the left and one above, that deviate from this. The group to the left most probably represents surface water, whilst the one above is probably due to man made structures such as concrete farmyards, etc. which would appear warmer than the surounding vegetation and have a lower vegetation index.

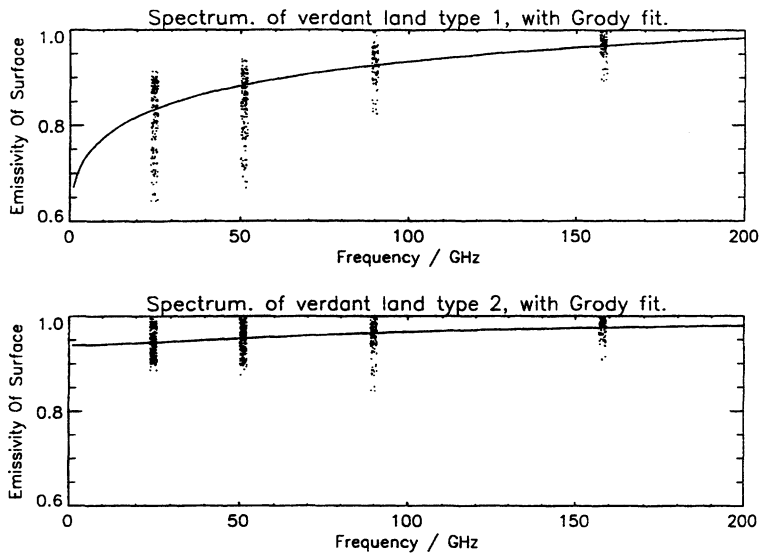

Figure 7. Spectra for the two verdant land types, with overplotted Grody fits.

Land type two can probably be described by means of mixing the emissivites for free water and dense crop in such a way as to fit its spectra. The usefulness of this would depend on how the amount of free water changed with time. If it changed in relatively random way of short periods of time, which is conceiveable, it would obviuosly not be of much use. But if the degree of irrigation were quite constant such a scheme should work.

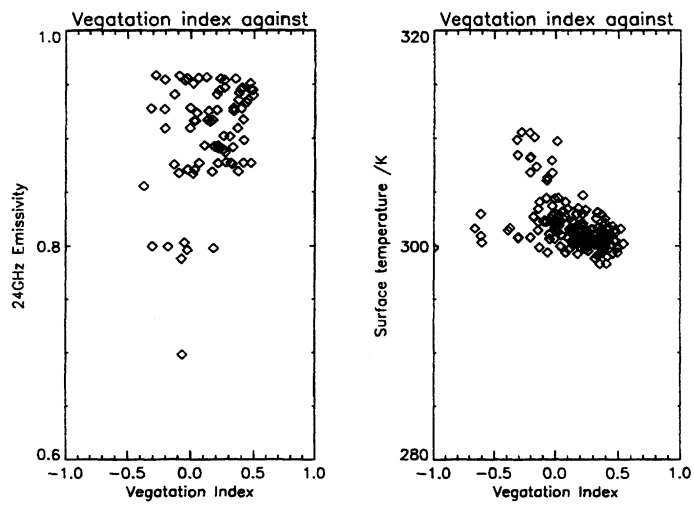

Figure 8. Plots of vegetation index against 24GHz emissivity and surface temperature for the verdant sites.

7. GRODY PARAMATIZATION

Grody sugested a method of paramatizing the microwave emissivity of a surface (see ref (7)) at any frequency in terms of its emissivity at frequencies of zero,ϵ_0, and infinty, ϵ_∞, ;an intermediate frequency ,ν_t; and a rate of change, κ. The equation below shows Grodys sugested paramatization,

$$\epsilon_\nu = \frac{\epsilon_0 + \epsilon_\infty (\frac{\nu}{\nu_t})^\kappa}{1 + (\frac{\nu}{\nu_t})^\kappa} \tag{2}$$

A least squares fit can be done to this equation from the averages of the emissivities for each frequency in a spectrum, and hence the parameters can be calculated. This method is well suited to satellite profile retreival because of its simplicity, low computational costs and preservation of informational content in retreivals.

How ever the fits that were used in the report were poorly constrained msot probably due to the slowly varrying nature of the spectra.

8. CONCLUSION

Microwave spectra and measured emissivities for an arid site in the Crau region of France have been presented. The emissivities were found to be comparable with those for bare soil sites that have been measured with the same radiometers on other campaigns (see ref (8)) , though the 157GHz is slightly lower due to the effect of cloud. The effect of variation in the typical vegetation conditions found in the region was investigated and found to have an effect on the emissivity, though there was little change in the vegetation index as measured.

The spectra and measured emissivities for rice paddies and other verdant crops were presented. The effect of heavy irrigation is readily apparent from the two sets of data and a possible means of representing this as a simple mixing of crop, an essentailly black surface, and water was discussed. The emissivities sensitivity to crop density was investigated and though no trends could be discerned this was probably due to too small a variation in crop density.

The use of modelled zenith brightness temperatures, at a range of frequencies, to the calculation of surface emissivities in a real experiment has been explored, and the problems associated with it have been highlighted.

9. ACKNOWLEDGEMENTS

The author would like to thank Dave Offiler for organising the experiment and Dave Jones and Steve English for organising the microwave side of things. The author would like to thank Tim Hewison for his help on all things radiometeric ,the ground and R.A.F crew of the UKMO C-130, the scientists that took part, especially Dvaid Pick for operating MARSS and Deimos under difficult conditions, and those responsible for the design and upkeep of the MARSS and Deimos radiometers.

10. REFERENCES

[1] T.J.Hewison . The design of Deimos: a microwave radiometer with channels at 23,8 and 50.3GHz for the UK Met. research flught C-130. Proceeding IGARSS '95, pp (2261-3)

[2] S.J.English et al. Aircraft measurements of water vapour continuum absorption at millimetre wavelengths. Quaterly journal of the meteorologiacl society, vol(120), pp (603-625), 1994

[3] T.J.Hewison Ground based experiment to validate atmospheric oxygen transmission models, UK Met.0(RS) working paper no. 111.

[4] T.J.Hewison Results of microwave airborne campaigns over snow and ice. UK Met.0(RS) working paper no. 19

[5] A.J.LaRocca The infrared and electro-optical systems handbook, vol(1) ,Artificial Sources. pp (112), 1993

[6] J.Morlan A ground based experiment to measure the microwave emisivities of soils and vegetation under both wet and dry conditions. A Personal communication

[7] N.C.Grody Surafce identification using satellite radiometers IEEE tarns. Geoscince and Remote sensing, vol(26), pp (850-9), 1988.

[8] S.J.English and T.J.Hewison Measurements at 23.8, 50.1, 89.0 and 157.0 GHz over the NOPEX test site during Spetember 1995. UK Met.O(rs) Branch working paper no. 20